Sensors and Materials, Vol. 37, No. 2 (2025) 587–592
MYU Tokyo

S & M 3938

Sm-doped $CaHfO_3$ Single-crystal Scintillators

Yusuke Endo,* Kensei Ichiba, Daisuke Nakauchi,
Takumi Kato, Noriaki Kawaguchi, and Takayuki Yanagida

Nara Institute of Science and Technology, Takayama, Ikoma, Nara 630-0192, Japan

(Received October 23, 2024; accepted December 12, 2024)

Keywords: X-ray detection, photoluminescence, floating zone method, afterglow

In the present study, we investigated the photoluminescence (PL) and scintillation properties of Sm:$CaHfO_3$. All Sm:$CaHfO_3$ samples showed multiple PL emission peaks due to the 4f–4f transitions of Sm^{3+}. Additionally, the PL quantum yield of 0.5% Sm:$CaHfO_3$ was 62.8% under excitation at 410 nm, and the value was the highest among the samples. Under X-ray irradiation, all the samples showed emission peaks due to the 4f–4f transitions of Sm^{3+}. Afterglow levels at 20 ms after 2 ms X-ray irradiation were 6000–22000 ppm.

1. Introduction

A scintillator can instantly convert ionizing radiations such as X- and γ-rays into numerous low-energy photons (scintillation photons). Scintillation photons are converted to an electrical signal by a photodetector like a Si photodiode (Si-PD).[1,2] This measurement system is used in radiation detectors in security[3–5] and medical[6] applications. In particular, airport baggage screening devices and X-ray flat panel detectors are integrated-type detectors that measure scintillation intensity by integrating scintillation signals over a certain time. Scintillators designed for integrated-type detectors require large effective atomic number (Z_{eff}), high density to enhance the probability of interaction with X-rays,[7] high scintillation intensity, high chemical stability for long-term use, and low afterglow level (AL). $CdWO_4$ (CWO) and Tl:CsI single-crystal scintillators are currently used in integrated-type detectors. However, CWO contains Cd, a toxic substance, and Tl:CsI shows small deliquescence and relatively high AL. As a result, alternative materials are being sought in various material forms such as single crystals,[8–26] ceramics,[8,19,27–30] and glasses.[31–41]

$CaHfO_3$ has large Z_{eff} (65.2), high density (6.95 g/cm^3), and high chemical stability. Up to now, scintillation properties of various rare-earth-doped (Ce^{3+},[42] Eu^{3+},[43] Tb^{3+},[44,45] Dy^{3+},[46] and Tm^{3+}[47]) $CaHfO_3$ single crystals have been evaluated, and Dy:$CaHfO_3$ showed a high light yield (*LY*) of 20000 photons/MeV. Therefore, $CaHfO_3$ single crystal is an excellent host for testing a new scintillator. Sm^{3+} exhibits several emission peaks within 500–700 nm, matching the sensitivity of the Si-PD typically used in general integrated-type detectors. In the present

*Corresponding author: e-mail: endo.yusuke.ey5@ms.naist.jp
https://doi.org/10.18494/SAM5432

ISSN 0914-4935
https://myukk.org/

study, we investigated the scintillation and photoluminescence (PL) properties of Sm:$CaHfO_3$ single crystals.

2. Experimental Setups

CaO (99.99%), HfO_2 (99.95%), and Sm_2O_3 (99.99%) were used as starting materials. The amount of CaO was increased by 10% above the stoichiometric ratio,[42] and the concentrations of Sm were 0.05, 0.1, 0.5, 1.0, and 2.0%. Crystals were grown in the same manner as in a previous study.[42] The less cracked portions of the crystallized rods were selectively divided and polished using a grinder polisher (Buehler, MetaServ 250) to prepare samples for evaluation.

Powder X-ray diffraction (PXRD) patterns were observed using an X-ray diffractometer (Rigaku, MiniFlex 600). PL excitation and emission spectra and PL quantum yield (*QY*) were measured using Quantaurus-QY (Hamamatsu Photonics, C11347). PL decay curves were evaluated using Quantaurus-τ (Hamamatsu Photonics, C11367). X-ray-induced scintillation spectra, decay curves, and ALs were measured using our original experimental setups.[48,49]

3. Results and Discussion

Crystals were successfully grown, and single crystalline rods were obtained. From these rods, some parts were selected for polishing, and after polishing, the length, width, and thickness of the samples were determined to be 2, 2–4, and 0.6 mm, respectively. The samples appeared colorless and transparent. Except for these polished parts, the remaining parts were crushed for XRD measurements. The PXRD patterns of all the samples were almost the same as those of the rare-earth-doped $CaHfO_3$ single crystals synthesized by our research group.[42–47] The patterns were consistent with the reference pattern of $CaHfO_3$ (International Crystallographic Diffraction Data No. 36-1473), and no extra peaks were detected. Therefore, the samples have a single-phase structure of $CaHfO_3$, which belongs to the Pnma space group of the orthorhombic structure.[50,51]

Figure 1 shows the PL excitation and emission spectra of the 1.0% Sm:$CaHfO_3$ sample as a representative. The vertical and horizontal axes of the spectrum indicate excitation and emission wavelengths, respectively. All the samples exhibited several emission peaks derived from the

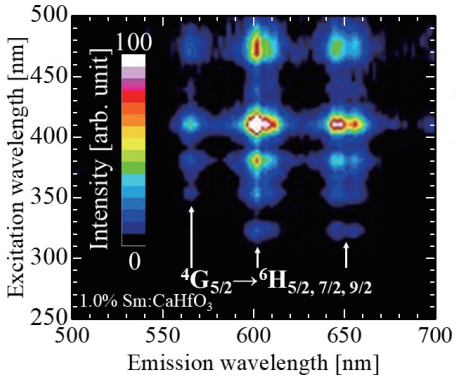

Fig. 1. (Color online) PL spectrum of 1.0% Sm:$CaHfO_3$ sample.

4f–4f transitions of Sm^{3+}.[52] The PL *QY* values of all the samples were evaluated under excitation at 410 nm and accumulating signals at 500–680 nm. The *QY* values ranged from 18.3 to 62.8% depending on Sm concentration. Figure 2 shows the PL decay curves of the samples. The decay curves were measured under excitation ($\lambda_{Ex.}$) at 410 nm and monitoring ($\lambda_{Em.}$) at 600 nm and approximated using a single exponential function. The obtained decay time constants ranging from 1.0 to 1.3 ms are similar to those of Sm-doped materials previously reported;[53,54] thus, the constants would be due to the 4f–4f transitions of Sm^{3+}. On the basis of the *QY* values and decay time constants, the radiative (k_f) and nonradiative (k_{nr}) transition rates were calculated and are listed in Table 1. As the concentration of Sm increased from 0.5 to 2.0%, k_f decreased and k_{nr} increased, indicating that concentration quenching occurred in the 1.0 and 2.0% Sm:$CaHfO_3$ samples.

Figure 3 shows the X-ray-induced scintillation spectra of the samples. The spectra showed emission peaks originating from the 4f–4f transitions of Sm^{3+}.[55,56] Figure 4 shows the X-ray-induced decay curves of the samples. The decay curves were approximated using a single exponential function with decay time constants of 1.2–1.5 ms except for instrumental response functions (IRFs). These decay time constants would be due to the 4f–4f transitions of Sm^{3+} according to the results of PL decay curves. Following these scintillation properties, the AL was evaluated. AL values at Sm concentrations of 0.05, 0.1, 0.5, 1.0, and 2.0% at 20 ms after 2 ms of X-ray irradiation were determined to be 22000, 12000, 11000, 10000, and 6000 ppm,

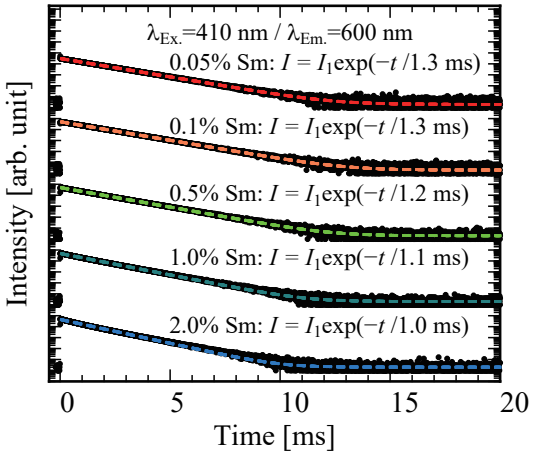

Fig. 2. (Color online) PL decay curves of all samples.

Table 1
PL properties of Sm:$CaHfO_3$ samples.

Sample	*QY* (%)	Decay time constant (ms)	k_f (s^{-1})	k_{nr} (s^{-1})
0.05% Sm:$CaHfO_3$	18.3	1.3	140	630
0.1% Sm:$CaHfO_3$	27.4	1.3	210	560
0.5% Sm:$CaHfO_3$	62.8	1.2	520	310
1.0% Sm:$CaHfO_3$	55.6	1.1	510	400
2.0% Sm:$CaHfO_3$	44.1	1.0	440	560

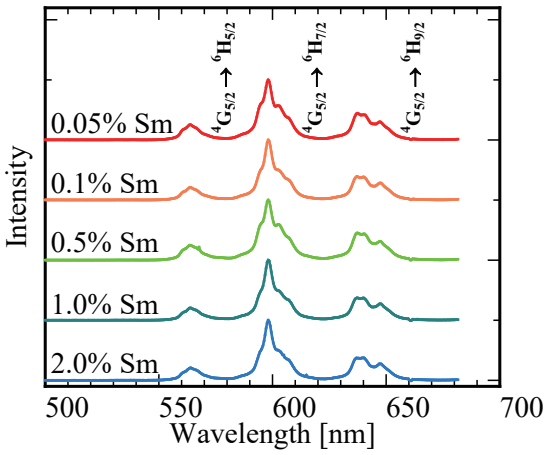

Fig. 3. (Color online) Scintillation spectra.

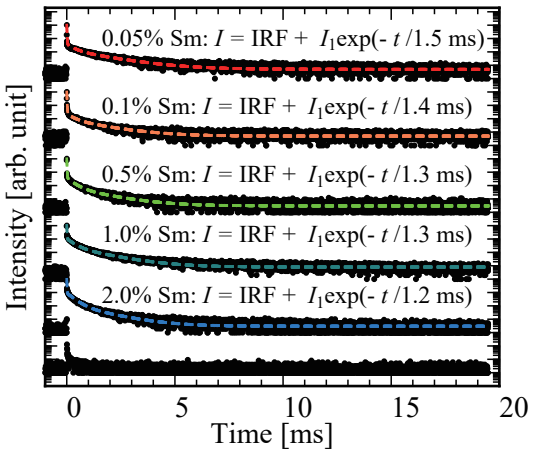

Fig. 4. (Color online) Scintillation decay curves.

respectively. These AL values were somewhat higher than those of the commercial scintillators for integrated-type detectors, such as CWO (~10 ppm) and Tl:CsI (~300 ppm).[49] HfO_2 is widely recognized as a phosphorescent material,[57] and a small amount of remaining HfO_2 may act as a source of afterglow. Given that the AL decreased with increasing Sm concentration, it is possible that Sm decreased the AL in $CaHfO_3$. This requires further study. Owing to their high AL, the application of Sm:$CaHfO_3$ to airport baggage screening devices is not feasible. However, they may be suitable for use in radiography devices with inspection intervals long enough to eliminate the impact of afterglow.

4. Conclusions

0.05, 0.1, 0.5, 1.0, and 2.0% Sm:$CaHfO_3$ single crystals were synthesized by the FZ method, and their PL and scintillation properties were evaluated. In the PL and scintillation spectra, all the samples showed emission peaks originating from the 4f–4f transitions of Sm^{3+}. The PL *QY* of the 0.5% Sm:$CaHfO_3$ sample was 62.8% under excitation at 410 nm, and this value was the highest among all the samples. In afterglow curves, the obtained AL values were within the 6000–22000 ppm range and rather higher than those of commercial scintillators, CWO and Tl:CsI. Considering all the PL and scintillation results, the application of Sm:$CaHfO_3$ single crystals to airport baggage screening devices in the security field is difficult, but they have potential for use in radiography devices like chest X-ray examination devices.

Acknowledgments

This work was supported by MEXT Grants-in-Aid for Scientific Research A (22H00309), Scientific Research B (23K21827, 23K25126, and 24K03197), and Exploratory Research (22K18997), Asahi Glass Foundation, and Suzuki Foundation.

References

1 K. Watanabe: Jpn. J. Appl. Phys. **62** (2023) 010507.
2 T. Yanagida, T. Kato, D. Nakauchi, and N. Kawaguchi: Jpn. J. Appl. Phys. **62** (2023) 010508.
3 C. W. E. van Eijk: Nucl. Instrum. Methods Phys. Res., Sect. A **460** (2001) 1.
4 T. K. Lewellen: Phys. Med. Biol. **53** (2008) R287.
5 C. Greskovich and S. Duclos: Annu. Rev. Mater. Sci. **27** (1997) 69.
6 G. Harding: Radiat. Phys. Chem. **71** (2004) 869.
7 A. Ito and S. Matsumoto: Jpn. J. Appl. Phys. **62** (2023) 010612.
8 T. Yanagida, T. Kato, D. Nakauchi, and N. Kawaguchi: Sens. Mater. **36** (2024) 443.
9 K. Ichiba, T. Kato, D. Nakauchi, N. Kawaguchi, and T. Yanagida: Sens. Mater. **36** (2024) 451.
10 T. Kunikata, P. Kantuptim, D. Shiratori, T. Kato, D. Nakauchi, N. Kawaguchi, and T. Yanagida: Sens. Mater. **36** (2024) 457.
11 H. Kimura, H. Fukushima, K. Watanabe, T. Fujiwara, H. Kato, M. Tanaka, T. Kato, D. Nakauchi, N. Kawaguchi, and T. Yanagida: Sens. Mater. **36** (2024) 507.
12 K. Miyazaki, D. Nakauchi, T. Kato, N. Kawaguchi, and T. Yanagida: Sens. Mater. **36** (2024) 515.
13 K. Yamabayashi, K. Okazaki, D. Nakauchi, T. Kato, N. Kawaguchi, and T. Yanagida: Sens. Mater. **36** (2024) 523.
14 T. Yanagida, K. Watanabe, T. Kato, D. Nakauchi, and N. Kawaguchi: Sens. Mater. **35** (2023) 423.
15 H. Fukushima, D. Nakauchi, T. Kato, N. Kawaguchi, and T. Yanagida: Sens. Mater. **35** (2023) 429.
16 D. Shiratori, H. Fukushima, D. Nakauchi, T. Kato, N. Kawaguchi, and T. Yanagida: Sens. Mater. **35** (2023) 439.
17 P. Kantuptim, T. Kato, D. Nakauchi, N. Kawaguchi, K. Watanabe, and T. Yanagida: Sens. Mater. **35** (2023) 451.
18 K. Okazaki, D. Nakauchi, H. Fukushima, T. Kato, N. Kawaguchi, and T. Yanagida: Sens. Mater. **35** (2023) 459.
19 D. Nakauchi, F. Nakamura, T. Kato, N. Kawaguchi, and T. Yanagida: Sens. Mater. **35** (2023) 467.
20 N. Kawaguchi, T. Kato, D. Nakauchi, and T. Yanagida: Jpn. J. Appl. Phys. **62** (2023) 010611.
21 Y. Fujimoto and K. Asai: Jpn. J. Appl. Phys. **62** (2023) 010605.
22 D. Nakauchi, T. Kato, N. Kawaguchi, and T. Yanagida: Jpn. J. Appl. Phys. **62** (2023) 010607.
23 T. Suto, N. Kawano, K. Okazaki, Y. Takebuchi, H. Fukushima, T. Kato, D. Nakauchi, and T. Yanagida: Jpn. J. Appl. Phys. **62** (2023) 010610.
24 R. Nagaoka, N. Kawano, Y. Takebuchi, H. Fukushima, T. Kato, D. Nakauchi, and T. Yanagida: Jpn. J. Appl. Phys. **61** (2022) 110601.
25 M. Koshimizu: Jpn. J. Appl. Phys. **62** (2023) 010503.
26 H. Fukushima, D. Nakauchi, T. Kato, N. Kawaguchi, and T. Yanagida: Jpn. J. Appl. Phys. **62** (2023) 010506.
27 H. Fukushima, D. Nakauchi, T. Kato, N. Kawaguchi, and T. Yanagida: Sens. Mater. **36** (2024) 489.
28 T. Kato, D. Nakauchi, N. Kawaguchi, and T. Yanagida: Sens. Mater. **36** (2024) 531.
29 T. Kunikata, T. Kato, D. Shiratori, P. Kantuptim, D. Nakauchi, N. Kawaguchi, and T. Yanagida: Sens. Mater. **35** (2023) 491.
30 Y. Shao, R. L. Conner, N. R. S. Souza, R. S. Silva, and L. G. Jacobsohn: Jpn. J. Appl. Phys. **62** (2023) 010601.
31 D. Nakauchi, H. Kimura, D. Shiratori, T. Kato, N. Kawaguchi, and T. Yanagida: Sens. Mater. **36** (2024) 573.
32 Y. Takebuchi, A. Masuno, D. Shiratori, K. Ichiba, A. Nishikawa, T. Kato, D. Nakauchi, N. Kawaguchi, and T. Yanagida: Sens. Mater. **36** (2024) 579.
33 K. Okazaki, D. Nakauchi, A. Nishikawa, T. Kato, N. Kawaguchi, and T. Yanagida: Sens. Mater. **36** (2024) 587.
34 N. Kawaguchi, K. Watanabe, D. Shiratori, T. Kato, D. Nakauchi, and T. Yanagida: Sens. Mater. **35** (2023) 499.
35 Y. Takebuchi, D. Shiratori, T. Kato, D. Nakauchi, N. Kawaguchi, and T. Yanagida: Sens. Mater. **35** (2023) 507.
36 H. Kimura, T. Fujiwara, M. Tanaka, T. Kato, D. Nakauchi, N. Kawaguchi, and T. Yanagida: Sens. Mater. **35** (2023) 513.
37 Y. Oshima, K. Watanabe, H. Shiga, and G. Wakabayashi: Sens. Mater. **35** (2023) 545.
38 H. Masai and T. Yanagida: Jpn. J. Appl. Phys. **62** (2023) 010606.
39 D. Shiratori, H. Fukushima, D. Nakauchi, T. Kato, N. Kawaguchi, and T. Yanagida: Jpn. J. Appl. Phys. **62** (2023) 010608.
40 N. Wantana, E. Kaewnuam, Y. Tariwong, N. D. Quang, P. Pakawanit, C. Phoovasawat, N. Vittayakorn, S. Kothan, H. J. Kim, and J. Kaewkhao: Jpn. J. Appl. Phys. **62** (2023) 010602.
41 K. Shinozaki, G. Okada, N. Kawaguchi, and T. Yanagida: Jpn. J. Appl. Phys. **62** (2023) 010603.
42 H. Fukushima, D. Nakauchi, T. Kato, N. Kawaguchi, and T. Yanagida: J. Lumin. **250** (2022) 119088.
43 Y. Endo, K. Ichiba, D. Nakauchi, T. Kato, N. Kawaguchi, and T. Yanagida: Sens. Mater. **36** (2024) 473.
44 Y. Endo, K. Ichiba, D. Nakauchi, H. Fukushima, K. Watanabe, T. Kato, N. Kawaguchi, and T. Yanagida: Solid State Sci. **145** (2023) 107333.

45 Y. Endo, K. Ichiba, D. Nakauchi, K. Watanabe, T. Kato, N. Kawaguchi, and T. Yanagida: Opt. Mater. **152** (2024) 115524.
46 Y. Endo, K. Ichiba, D. Nakauchi, K. Okazaki, K. Watanabe, T. Kato, N. Kawaguchi, and T. Yanagida: Opt. Mater. **157** (2024) 116276.
47 Y. Endo, K. Ichiba, D. Nakauchi, T. Kato, N. Kawaguchi, and T. Yanagida: Jpn. J. Appl. Phys. **63** (2024) 062003.
48 T. Yanagida, K. Kamada, Y. Fujimoto, H. Yagi, and T. Yanagitani: Opt. Mater. **35** (2013) 2480.
49 T. Yanagida, Y. Fujimoto, T. Ito, K. Uchiyama, and K. Mori: Appl. Phys. Express **7** (2014) 062401.
50 A. Feteira, D. C. Sinclair, K. Z. Rajab, and M. T. Lanagan: J. Am. Ceram. Soc. **91** (2008) 893.
51 Y. M. Ji, D. Y. Jiang, Z. H. Wu, T. Feng, and J. L. Shi: Mater. Res. Bull. **40** (2005) 1521.
52 K. Ichiba, G. Okada, Y. Takebuchi, T. Kato, D. Shiratori, D. Nakauchi, N. Kawaguchi, and T. Yanagida: J. Lumin. **257** (2023) 119698.
53 E. Malchukova and B. Boizot: J. Lumin. **229** (2021) 117662.
54 A. Nishikawa, D. Shiratori, T. Kato, D. Nakauchi, N. Kawaguchi, and T. Yanagida: Sens. Mater. **36** (2024) 597.
55 T. Kunikata, K. Watanabe, P. Kantuptim, T. Kato, D. Nakauchi, N. Kawaguchi, and T. Yanagida: Nucl. Instrum. Methods Phys. Res., Sect. B **546** (2024) 165172.
56 R. Yu, H. Mi Noh, B. Kee Moon, B. Chun Choi, J. Hyun Jeong, H. Sueb Lee, K. Jang, and S. Soo Yi: J. Lumin. **145** (2014) 717.
57 D. A. Pejaković: J. Lumin. **130** (2010) 1048.